Performance of Coherent Impulse Radio and Multiband-OFDM on IEEE UWB Channels

Matts-Ola Wessman, Arne Svensson
Communication System Group, Department of Signals and Systems,
Chalmers University of Technology, SE-412 96 Gothenburg, Sweden
Email: {matts-ola.wessman, arne.svensson}@s2.chalmers.se

Abstract— **This paper presents the performance of single band impulse radio systems, TH-UWB and DS-UWB, multiband impulse radio systems, MB-UWB, and multiband OFDM systems on the IEEE 802.15 UWB channel models CM1–CM4.**

The investigated impulse radio systems use approximately the spectrum 3–6 GHz and have a data rate around 100 Mbps. The DS-UWB system with a fractionally spaced Rake receiver with 10 fingers performs better than the MB-UWB system with a chip-spaced Rake receiver with one finger in each of the six bands. However, the sampling frequencies after the pulse matched filter for the DS-UWB and MB-UWB systems are 20 and 0.250 GHz, respectively.

The uncoded data rate of the multiband-OFDM system, which uses 3 bands of 500 MHz in 3.1-4.6 GHz, is 812 Mbps. The performance of uncoded multiband-OFDM systems on CM1–CM4 without shadowing is equal to the perfomance of the same modulation on a Rayleigh fading channel. The performance of the coded multiband-OFDM systems on CM1 is worse than on CM4, and the performance on CM4 is worse than on an uncorrelated Rayleigh fading channel.

I. Introduction

In the near future, there will appear a demand for low cost, high-speed, wireless links for short range (< 10 m) communication. Such links should support digital video transmission to be able to replace impractical cables. Ultra-wideband (UWB) systems with data rates of several hundred megabits per second could provide those features.

UWB systems can be divided into two groups: single band and multiband. Two commonly used single-band impulse radio systems are time-hopping spread-spectrum impulse radio (TH-UWB) and direct-sequence spread-spectrum impulse radio (DS-UWB). In DS-UWB, the pulses are transmitted continuously using a pseudorandom sequence for the spreading of information bits, and in TH-UWB, a pseudorandom sequence defines the time when the pulses are transmitted [1].

Multiband-UWB and multiband-OFDM divide the spectrum into several bands, [2]–[4]. Multiband-UWB uses impulse radio to transmit pulses in all bands. By setting the pulse repetition period in each band to be longer than the channel delay spread, we can have a system with negligible interpulse interference. However, high data rates are achieved since all bands are used in parallel. On the other hand, multiband-OFDM systems transmit one OFDM symbol in the first band, then in the second, etc. Multiband-OFDM was proposed for the physical layer within IEEE 802.15.3 that covers UWB communication in a wireless personal area network (WPAN).

Recently, IEEE proposed a channel model for UWB systems [5] based on the Saleh–Valenzuela model where multipath components arrive in clusters [6]. In general, several multipath components arrive during the duration of one pulse, which generates intrapulse interference. Before this channel model, previous research on ultra-wideband focused on the AWGN channel or simple multipath channels where taps are spaced at integer multiples of one pulse period. Also a shift from single-band to multiband systems have been seen.

The objective of this paper is to summarize some results on the performance of four coherent systems TH-UWB, DS-UWB, MB-UWB and multiband-OFDM on the IEEE UWB channel model that can be found in [7]–[10]. The multiband-OFDM system will be coded and using the channel model without shadowing. The other three systems will only use repetition coding and include shadowing. All systems will also have different data rate.

II. Impulse Radio

A. Single-Band TH-UWB and DS-UWB Impulse Radio

In TH-UWB, the transmitted signal $s_{\mathrm{TH}}(t)$ for one user using binary antipodal modulation can be defined as [1]

$$s_{\mathrm{TH}}(t) = a_{\mathrm{TH}} \sum_{j=-\infty}^{\infty} w_{\mathrm{tr}}(t - jT_f - c_jT_m)(1 - 2D_{\lfloor j/N_{\mathrm{TH}} \rfloor}) \quad (1)$$

where $w_{\mathrm{tr}}(t)$ denotes the transmitted pulseform that has a maximum amplitude of one, a duration of T_m and is transmitted with a repetition period T_f. The position of a transmitted pulse within each repetition period is determined by a pseudorandom code c_j which selects one of the N_h slots, each having a duration of T_m. The pseudorandom code c_j takes integer value between 0 and $N_h - 1$ and it is assumed that $T_f \geqslant N_h T_m$.

Moreover, a_{TH} is the maximum amplitude of the TH-UWB pulse train. $D \in \{0, 1\}$ is a data stream and $\lfloor x \rfloor$ denotes the integer part of x. A new bit starts with $j \equiv 0 \pmod{N_{\mathrm{TH}}}$. Each bit is transmitted with N_{TH} pulses and has a duration of $T_b = N_{\mathrm{TH}} T_f$.

A DS-UWB system is basically identical to an ordinary DS-SS system except that the bandwidth spreading effect is achieved by pulse shaping. Similar to (1) above, DS-UWB is defined as

$$s_{\mathrm{DS}}(t) = a_{\mathrm{DS}} \sum_{j=-\infty}^{\infty} w_{\mathrm{tr}}(t - jT_m) n_j (1 - 2D_{\lfloor j/N_{\mathrm{DS}} \rfloor}) \quad (2)$$

where n_j is a pseudorandom code that takes values $\{\pm 1\}$ and a_{DS} is the maximum amplitude of the DS-UWB pulse train. Each bit consists of N_{DS} pulses and has a duration of $T_b = N_{\text{DS}} T_m$. The periods of the scrambling sequences c_j and n_j, used in TH-UWB and DS-UWB, are not less than N_{TH} and N_{DS}, respectively.

For the same bit rate, the processing gain for both binary TH-UWB and DS-UWB is defined as T_b/T_m. In the case of DS-UWB, the processing gain is equal to a repetition gain N_{DS}. In the TH-UWB, the processing gain consists of a repetition gain N_{TH} and a duty cycle gain T_f/T_m.

B. Multiband MB-UWB Impulse Radio

The multiband-UWB system is similar to the DS-UWB system above but with two main differences. The available signaling band is divided into N_{band} bands by using N_{band} pulses $\{w_b(t)\}$. The puls in band b can be defined as

$$w_b(t) = \sin(\pi t/T_m)\sin(2\pi f_b t) \quad \text{for} \quad 0 \leqslant t \leqslant T_m \tag{3}$$

where the frequencies $\{f_b\}$ are selected so that the pulses are almost pairwise orthogonal. The data stream D is transmitted consecutively in band $b \equiv j \pmod{N_{\text{band}}}$. The transmitted signal can be written as

$$s_{\text{MB}}(t) = a_{\text{MB}} \sum_{j=-\infty}^{\infty} w_b(t - jT_{\text{pab}}) n_j (1 - 2D_{\lfloor j/N_{\text{MB}} \rfloor}) \tag{4}$$

where a_{MB} is the maximum amplitude and $T_{\text{pab}} \geqslant T_m$ is the time between two pulses in adjacent bands. The pulse repetition period in one band is $T_f = N_{\text{band}} T_{\text{pab}}$. When $T_f - 2T_m$ is larger than the delay spread of the channel, no interchip interference is created between two chips in the same band. Each bit consists of N_{MB} pulses and the bit rate is given with $N_{\text{band}}/T_f/N_{\text{MB}}$. The duty cycle gain is T_f/T_m.

C. Impulse Radio Transceiver Algorithm

1) Coherent Detection: For TH-UWB, DS-UWB and MB-UWB, we investigate coherent, selective Rake-N receivers. In one band, the output from a pulse-matched filter is sampled at a given rate which is equal to symbol, chip, or a fraction of the chip rate. Based on the sampled signal, the delays, amplitudes, and phases of several multipath components are estimated. In the next step, the components or so-called 'fingers' having the N largest amplitudes are selected. The signals of the selected fingers are coherently added according to maximum ratio combining. The MB-UWB system has to have as many channel estimators and Rake receivers as there are bands. However, the number of Rake fingers and the sampling frequency can be reduced when the number of bands increase.

2) Channel Estimation: In our system, we use a data-aided (DA) approach that is based on using N_p known pilot bits per band in each packet to estimate the channel impulse response. All pilot bits are transmitted in the beginning of the data packet. Based on these pilots, the channel is estimated, and the rest of the packet is decoded based on the acquired channel characteristics.

Two suboptimal channel estimation algorithms with reduced complexity are used for TH-UWB and DS-UWB. The first one is the well known sliding window (SW) algorithm [13] and the second one is denoted the successive cancellation (SC) algorithm [14]. In the MB-UWB, the sliding window algorithm is used.

III. Multiband-OFDM

The multiband-OFDM system divides the spectrum B_{tot} into N_{band} bands, each with a bandwidth of B. The OFDM symbol number o is then transmitted in band $b \equiv o \pmod{N_{\text{band}}}$. Each OFDM symbol has N_{st} subcarriers where the subcarrier bandwidth is defined as $B_s = B/N_{\text{st}}$. One OFDM symbol has a duration of $T_{\text{SYM}} = T_{\text{FFT}} + T_{\text{cp}} + T_{\text{GI}}$ where $T_{\text{FFT}} = 1/B_s$ is the DFT integration time, T_{cp} is the length of the cyclic prefix and T_{GI} is the guard interval. N_{SD} is the number of data subcarriers per OFDM symbol. In total there are $K = N_{\text{band}} N_{\text{st}}$ subcarriers in all bands.

Under the assumptions that the cyclic prefix is long enough, no doppler shift and linear hardware, the subcarriers become independent. Then the received signal on subcarrier k can be modeled, with complex baseband representation, as

$$R_k = S_k C_k + n_k \quad 0 \leqslant k \leqslant N_{\text{band}} N_{\text{st}} - 1 \tag{5}$$

where S_k is the transmitted quadrature modulated symbol, n_k is complex valued noise and C_k is the value of $C(f_k)$ in (8) at subcarrier frequency $f_k = f_0 + kB_s$. The investigated receiver uses coherent detection with perfect channel estimates and QPSK modulation, which gives

$$X_k = R_k C_k^* = S_k |C_k|^2 + n_k C_k^* \quad 0 \leqslant k \leqslant N_{\text{band}} N_{\text{st}} - 1 \tag{6}$$

where * denotes complex conjugate.

In the investigated multiband-OFDM system, the information bits are first coded. Then the encoded bits were written into a block interleaver columnwise and read out rowwise. Then the QPSK modulator creates the complex symbol number j that is transmitted on subcarrier $k \equiv j \pmod{N_{\text{band}} N_{\text{st}}}$.

Two convolutional codes with constraint length 7 and code rate 1/2 and 1/3 are tested. They are denoted (2,1,7) and (3,1,7), respectively, and have $d_{\text{free}} = 10$ and 15, respectively. The size of the block interleaver was 16 rows and 24 columns. Also the BCH(63,30) code, which can correct $t = 6$ errors, is tested with a block interleaver of 63 rows and 17 columns.

The IEEE UWB channel model is constant during the transmission of one packet and no time diversity is available within one packet. Fortunately, the channel is frequency selective which creates an opportunity to use error control coding to achieve frequency diversity.

IV. IEEE UWB Channel Model

The IEEE UWB channel model is based on the Saleh–Valenzuela model where multipath components arrive in clusters [5], [6]. This multipath channel can be expressed as

$$h(t) = Xc(t) = X \sum_{l \geqslant 0} \sum_{k \geqslant 0} \alpha_{k,l} \delta(t - T_l - \tau_{k,l}) \tag{7}$$

where the real-valued multipath gain is defined by $\alpha_{k,l}$ for cluster l and ray k. The lth cluster arrives at T_l and its kth ray arrives at $\tau_{k,l}$ which is relative to the first path in cluster l, i.e. $\tau_{0,l} = 0$. The amplitude $|\alpha_{k,l}|$ has a log-normal distribution and the phase $\angle\alpha_{k.l}$ is chosen from $\{0, \pi\}$ with equal probability. The expected value $\mathbb{E}\left(|\alpha_{k,l}|^2\right)$ is proportional to $\exp(-T_l/\Gamma - \tau_{k,l}/\gamma)$, where Γ and γ denote a cluster- and a ray-decay factor, respectively. The interarrival time between two clusters $T_{l+1} - T_l$ or two rays within one cluster $\tau_{k+1,l} - \tau_{k,l}$ is exponentially distributed. Clearly, the interarrival time between any two rays is not an integer multiple of the pulse duration. Log-normal shadowing is modeled with $X = 10^{n/20}$ where n has a normal distribution with mean $\mu = 0$ and standard deviation $\sigma_x = 3$. The expected energy of a generated channel impulse response $\mathbb{E}\left(|h(t)|^2\right)$ is equal to $\mathbb{E}\left(|X|^2\right) = 10^{\sigma_x^2 \ln(10)/200 + \mu/10} \approx 1.27 \approx 1.04$ dB.

There are four different models, CM1, CM2, CM3 and CM4, for different channel characteristics. These are presented in Table I. Note that in this article, the models are used both with or without the shadowing term X. The above models assume that the channel impulse response is constant during transmission of one packet if it is shorter than 200 μs. Moreover, channel realizations are assumed to be independent between packets.

TABLE I

THE IEEE UWB CHANNEL MODEL

Model Characteristic	CM1	CM2	CM3	CM4	unit
Distance	0-4	0-4	4-10		m
(Non-)line of sight	LOS	NLOS	NLOS	NLOS	

V. ANALYSIS OF CHANNEL MODEL

The mean excess delay $\bar{\tau}^{(i)}$, and the RMS delay spread $\sigma_\tau^{(i)}$ can be calculated for one realization i of $c^{(i)}(t)$. Then the average of $\bar{\tau}^{(i)}$ and $\sigma_\tau^{(i)}$, denoted $\bar{\tau}$ and $\bar{\sigma}_\tau$, can be numerically estimated with a large number of realizations $\{c^{(i)}(t)\}$. A rough estimate of the coherence bandwidth could be achieved, which is here defined as $B_c = 1/(6\bar{\sigma}_\tau)$. By dividing the coherence bandwidth with the subcarrier bandwidth B_s from the OFDM system, we get the number of correlated subcarriers. See Tab. II for estimated values where $B_s = 4.125 \cdot 10^6$ Hz.

TABLE II

ESTIMATED MODEL CHARACTERISTICS OF CM1 TO CM4

Estimated Characteristic	CM1	CM2	CM3	CM4	unit
Avg. mean excess delay $\bar{\tau}$	4.85	9.57	15.58	28.47	ns
Avg. RMS delay spread $\bar{\sigma}_\tau$	5.30	8.40	14.39	25.91	ns
Coh. bandw. $B_c = 1/(6\bar{\sigma}_\tau)$	31.5	19.8	11.6	6.43	MHz
$B_c/4.125 \cdot 10^6$	7.6	4.8	2.8	1.6	

The continuous time Fourier transform of $c(t)$ in (7) is

$$C(f) = \sum_{l \geqslant 0} \sum_{k \geqslant 0} \alpha_{k,l} e^{-j2\pi f(T_l + \tau_{k,l})}. \quad (8)$$

When the number of taps is large, the central limit theorem tells us that $C(f)$ will converge in distribution to $I + jQ$ where I and Q are normally distributed with zero mean and variance σ^2. The zero mean is due to the fact that $\mathbb{E}\left(\alpha_{k,l}\right) = \mathbb{E}\left(e^{-j2\pi f(T_l+\tau_{k,l})}\right) = 0$. Consequently, we expect that the performance of an uncoded OFDM system on CM1–CM4 is the same as on a Rayleigh fading channel with uniformly distributed phase. The amplitude of the Fourier transform $|H(f)| = X|C(f)|$ has a Suzuki distribution for each f since X is log-normally distributed. We have numerically verified, with high accuracy, that the estimated pdfs of $|C(f)|$ and $\angle C(f)$ are Rayleigh and uniformly distributed, respectively.

VI. SIMULATION ASSUMPTIONS AND PARAMETERS

Common assumptions for all results are:

- The synchronization is assumed to be perfect, which means that the arrival time of the first path in the receiver is assumed perfectly known.
- The effects of the antenna and other nonlinear hardware have been neglected.

A. Impulse Radio

The simulations for TH-UWB, DS-UWB and MB-UWB systems were done in the passband. The common parameters for the impulse radio results are:

- IEEE UWB channel model with shadowing.
- E_b is the average received energy per information bit before the pulse matched filter. The calculation considers the energy loss due to N_p pilot bits and and the channel energy $\mathbb{E}\left(|h(t)|^2\right) = 1.04$ dB.
- The modulation format is antipodal binary pulse amplitude modulation (BPAM).
- The spreading code is the maximum-length sequence with a period of $2^8 - 1$, which is longer than the spreading factor, i.e., we simulate a long-code system.
- The sampling frequency in the simulator of the analog parts, e.g., the channel model and pulse matched filters, was set to 20 GHz, which is higher than the Nyquist rate.

1) TH-UWB and DS-UWB: In addition to the impulse radio parameters above, the TH-UWB and DS-UWB simulations were conducted using the following set of parameters:

- The uncoded data rate R_b is 100 Mbits/s. The payload length N_l of one data packet is 1000 bits.
- The transmitted pulseshape $w_{\text{tr}}(t)$ is the fifth derivative of the Gaussian pulse with a duration T_m of 0.5 ns. The pulse has a -10 dB bandwidth between 2.5 and 6.8 GHz. The pulse rate or chip rate is equal to 2 Gpulses/s.
- The processing gain T_b/T_m of both the DS-UWB and TH-UWB systems is 13 dB. For DS-UWB, the repetition gain $N_{\text{DS}} = 13$ dB or 20 pulses/bit. TH-UWB has the duty cycle gain of $T_f/T_m = 7$ dB and the repetition gain $N_{\text{TH}} = 6$ dB or 4 pulses/bit.
- After the pulse matched filter, the sampling frequencies for the fractionally, chip-, and symbol-spaced receivers were 20 GHz, 2 GHz, and 100 MHz, respectively.

2) MB-UWB: In addition to the impulse radio parameters above, the MB-UWB simulations were conducted using the following set of parameters:

- There are $N_{\text{band}} = 6$ bands with center frequencies f_b equal to 3.35, 3.85, 4.35, 4.85, 5.35, and 5.85 GHz, respectively.
- The pulse duration T_m is 4 ns and the pulse repetition time T_f is 24 ns. The repetition gain N_{MB} is 2 and the duty cycle gain T_f/T_m is 6. The chip rate is 250 Mchips/s and the bit rate is 125 Mbps.
- The number of bits per packet N_{bit} is 2400 bits.
- The sampling rate after the pulse matched filter is 250 MHz and 20 GHz for the chip- and the fractionally spaced receiver, respectively.

B. Multiband-OFDM

The simulations of multiband-OFDM was performed using complex baseband representation in the frequency domain. The following parameters was used in the study:

- IEEE channel model without shadowing
- E_b is the energy per information bit is $\mathbb{E}\left(|S_k C_k|^2\right)/(R \log_2 M)$ where R is the code rate and $M = 4$ due to QPSK modulation. Notice that the energy loss due to pilots and cyclic prefix has not been considered.
- The number of information bits in one packet is around 2000 bits.
- Subcarrier bandwidth $B_s = 4.125 \cdot 10^6$ Hz and the subcarrier frequencies $f_k = 3.17 \cdot 10^9 + kB_s$ Hz.
- Number of bands $N_{\text{band}} = 3$.
- The T_{SYM} = 312.5 ns. $N_{\text{ST}} = N_{\text{SD}} = 128$ data carriers per OFDM symbol. Uncoded data rate of 812 Mbps.
- Band 0 has $0 \leqslant k \leqslant 127$; band 1 has $128 \leqslant k \leqslant 255$; band 2 has $256 \leqslant k \leqslant 383$.

VII. RESULTS

A. Single-Band DS-UWB and TH-UWB Impulse Radio

Fig. 1 presents the bit error rate of the DS-UWB system on the first IEEE-UWB channel model (CM1) with shadowing and with perfect knowledge of the channel characteristics and three versions of the Rake receiver with different number of fingers. The performance of the fractionally spaced Rake receiver is clearly the best and improves with an increasing number of fingers since more energy is effectively used in the receiver. The chip spaced (CS) Rake receivers perform much worse than the FS-Rake and the symbol spaced (SS) Rake receiver has catastrophically bad performance.

Fig. 2 presents the results of simulations of TH-UWB and DS-UWB systems with estimated channels CM1 to CM4. In all cases, the channels were estimated using the successive cancellation technique with 100 pilot bits. The detection was performed using a Rake-10 receiver. As one can see, there is no significant difference in BER between the DS-UWB and TH-UWB systems. However, the study has not taken into consideration the synchronization problems of the TH-UWB.

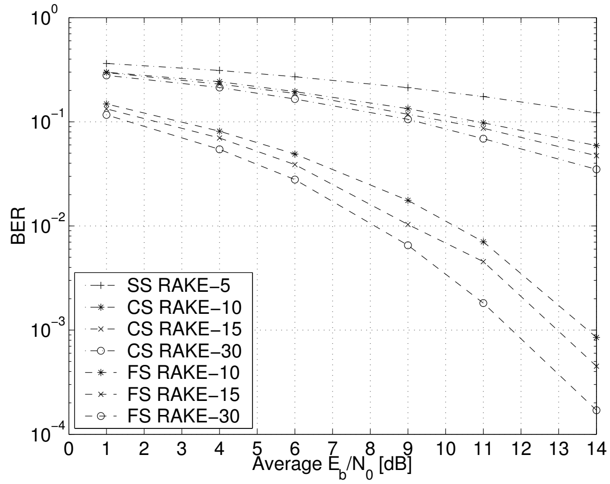

Fig. 1. The bit error rate of symbol-, chip-, and fractionally spaced Rake receivers with perfect channel estimation for DS-UWB on CM1 with shadowing.

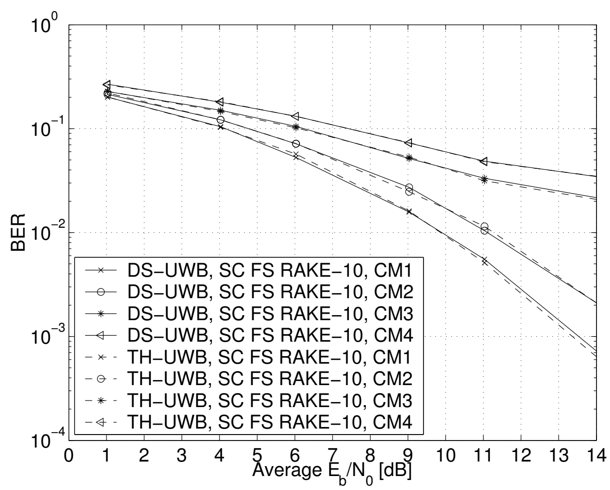

Fig. 2. The bit error rate of TH-UWB and DS-UWB with fractionally spaced Rake receivers using the successive cancellation algorithm and N_p = 100 pilot bits on CM1–CM4 with shadowing.

According to [7], 10 Rake fingers is a good trade-off between performance and complexity. However, the FS-Rake requires a sampling frequency of at least 14 GHz to avoid too large losses due to aliasing and intrapulse interference.

B. Multiband MB-UWB Impulse Radio

In order to reduce the sampling frequency, the multiband principle is appealing. An internal study [8] focused on MB-UWB with only 1 or 2 fingers per band and different channel estimators on the IEEE UWB channel model. Fig. 3 shows that the multiband chip-spaced and fractionally spaced Rake receivers, with a repetition code of length 2 and one Rake finger, have almost the same performance.

C. Multiband-OFDM

In Fig. 4, we see that the uncoded system on CM1 and CM4 without shadowing has the same performance as that

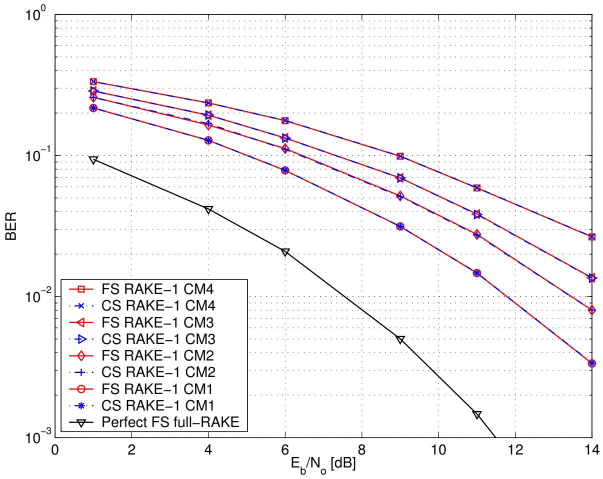

Fig. 3. The bit error rate of chip- and fractionally spaced Rake receivers with 1 finger and sliding window.

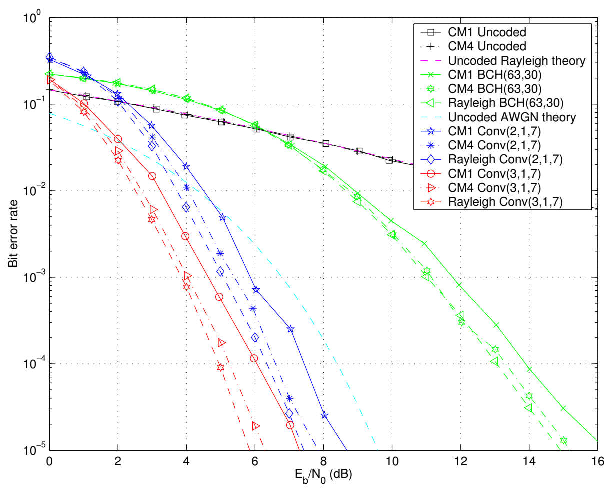

Fig. 4. The bit error rate of an uncoded system and with convolutional codes (2,1,7) and (3,1,7) and the BCH(63,30) code on IEEE channel models CM1 and CM4 without shadowing and uncorrelated Rayleigh fading.

system on flat Rayleigh fading channels. This agrees with our previous conclusion that the subcarrier channel gains, $\{|C(f)|\}$, have Rayleigh distributed amplitudes. The same figure shows that the two convolutional codes perform better than the BCH(63,30) code on CM1, CM4, and an uncorrelated Rayleigh fading channel.

The performance of the coded multiband-OFDM systems on CM1 is worse than on CM4, and the performance on CM4 is worse than on an uncorrelated Rayleigh fading channel.

VIII. Conclusions

The investigated impulse radio systems use roughly the same bandwidth, 3–6 GHz, and have almost the same bit rate 100 or 125 Mbps. The MB-UWB system, with one Rake finger in each of the six bands and a sampling frequency of 0.25 GHz, performs almost equally well, in many cases, as the the single band DS-UWB system. Remember that the DS-UWB system used a fractionally spaced Rake receiver and 10 fingers and a sampling frequency of 20 GHz.

The performance of uncoded multiband-OFDM systems on CM1–CM4 without shadowing is equal to the perfomance of the same modulation on a Rayleigh fading channel. Since the performance of the coded and interleaved system is still worse than the performance on an uncorrelated fading channel, further gains should be available with other interleavers.

The multiband-OFDM system was investigated using the channel without shadowing and no fair comparison with the impulse radio systems is feasible. However, the multiband-OFDM system seems to be more promising

Acknowledgment

The authors would like to thank the Centre of Wireless Communication (CWC) at University of Oulu for providing their UWB simulator that was used for TH-UWB and DS-UWB. This work has partly been funded by Ultrawaves, the Swedish Research Council, and PCC++. The authors would like to acknowledge the contributions from Dr. Erik Agrell, Rana Chebl, Yonas Djamianto, Vittorio Fougatsaro, and Henry.

References

[1] M. Z. Win and R. A. Scholtz, "Ultra-wide bandwidth time-hopping spread-spectrum impulse radio for wireless multiple-access communications," *IEEE Trans. Commun.*, vol. 48, pp. 679–689, Apr. 2000.

[2] M. Pendergrass,"Time Domain supporting text for 802.15.3 alternate physical layer proposal", IEEE P802.15-03/144r1, IEEE P802.15 Working Group for Wireless Personal Area Networks, Mar. 2003.

[3] G. Shor, "TG3a-Wisair-CFP-Presentation", IEEE P802.15-03/151r3, IEEE P802.15 Working Group for Wireless Personal Area Networks, May 2003.

[4] "Multi-band OFDM Physical Layer Proposal for IEEE 802.15 Task Group 3a", www.multibandofdm.org.

[5] J. Foerster et al., "Channel modeling sub-committee report final," *IEEE P802.15 Wireless Personal Area Networks, P802.15-02/490r1-SG3a*, Feb. 2003.

[6] A. Saleh and R. Valenzuela, "A statistical model for indoor multipath propagation," *IEEE Journal on Select. Areas Commun.*, vol. 5, pp. 128–137, Feb. 1987.

[7] B. Mielczarek, M.-O. Wessman and A. Svensson, "Performance of Coherent UWB Rake Receivers with Channel Estimators", *IEEE VTC'03 fall*, Oct. 2003.

[8] Henry and Y. Djamianto, "Performance of coherent receivers for a pulsed multiband transceiver," *M.Sc. thesis report Ex025/2004*, Signals and Systems, Chalmers Univ. of Technology, Sweden, 2004.

[9] R. Chebl and V. G. Fougatsaro "Performance of multiband-OFDM in IEEE UWB channel models," *M.Sc. thesis report*, Signals and Systems, Chalmers Univ. of Technology, Sweden, 2004.

[10] M.-O. Wessman, A. Svensson and E. Agrell, "Frequency Diversity Performance of Coded Multiband-OFDM Systems on IEEE UWB Channels, " *IEEE VTC'04 fall*, Sept. 2004. To appear.

[11] T. S. Rappaport, *Wireless communication, principles and practice*, Prentice-Hall, 2nd ed., 2002.

[12] J. G. Proakis, "Adaptive equalization for TDMA digital mobile radio," *IEEE Trans. Veh. Tech.*, vol. 40, no. 2, pp. 333–341, May 1991.

[13] J. G. Proakis, *Digital communications,* McGraw-Hill, 4th ed., 2001.

[14] A. A. D'Amico, U. Mengali, and M. Morelli, "Multipath channel estimation for the uplink of a DS-CDMA system," *IEEE Int. Conf. on Communication (ICC)*, vol. 1, pp. 16–20, 2002.